Journal of Power Sources 198 (2012) 112–116

Contents lists available at SciVerse ScienceDirect

Journal of Power Sources

journal homepage: www.elsevier.com/locate/jpowsour

Short communication

Microphase separated hydroxide exchange membrane synthesis by a novel plasma copolymerization approach

Chengxu Zhang[a,b], Jue Hu[a,*], Xiangke Wang[a], Hirotaka Toyoda[c], Masaaki Nagatsu[d], Xiaodong Zhang[a], Yuedong Meng[a]

[a] Institute of Plasma Physics, Chinese Academy of Sciences, P. O. Box 1126, Hefei, PR China
[b] Department of Modern Physics, University of Science and Technology of China, Hefei, PR China
[c] Department of Electrical Engineering and Computer Science, Nagoya University, Chikusa, Nagoya, Japan
[d] Nanovision Science Section, Graduate School of Science and Technology, Shizuoka University, Naka-ku, Hamamatsu, Japan

ARTICLE INFO

Article history:
Received 5 July 2011
Received in revised form
22 September 2011
Accepted 23 September 2011
Available online 1 October 2011

Keywords:
Fuel cell
Hydroxide exchange membrane
Microphase-separated structure
Plasma copolymerization
Ultra-thin films

ABSTRACT

Hydroxide exchange membrane (HEM) is the most important and key performance-limiting component of HEMFC. Plasma copolymerization is adopted to synthesize the hydroxide exchange membranes with microphase-separated structure. The X-ray photoelectron spectroscopy and Fourier transform infrared spectroscopy demonstrate that the quaternary ammonium groups can be successfully introduced into the polymer matrix in the plasma copolymerization process. The transmission electron microscope images reveal that plasma copolymerization allowed the generation and aggregation of ionic groups and the formation of ionic transport channels, leading to an excellent phase-separated morphology of the membrane. The plasma-copolymerized hydroxide exchange membranes possess excellent hydroxide ion conductivity, chemical and thermal stability, ultra-thin and mechanical integrity structure, as well as the ability of building an efficient three-phase-boundary, making them very exiting candidates for fuel cell applications.

1. Introduction

By employing a basic environment, hydroxide exchange membrane fuel cells (HEMFCs) enhance the reaction kinetics for both oxygen reduction and fuel oxidation, and circumvent the problems with low durability, serious corrosion and high costs of the platinum catalyst encountered in proton exchange membrane fuel cells (PEMFCs) which operate under acid conditions [1–4]. In addition, HEMFCs also offer fuel flexibility, inhibited fuel crossover from anode to cathode, thus making it possible to higher the fuel cell efficiency [2,5]. However, due to the low conductivity for the hydroxide exchange membranes (HEMs), the most important and the key performance-limiting component of HEMFC, HEMFC cannot yet compete with its basic analogue (PEMFC) [6,7]. Besides, the needs for HEMs with necessary thermal and chemical stability, ultra-thin structure, and solubility in low boiling point water-solute solvents to building an efficient three-phase-boundary are also key challenges in the development of HEMFCs.

More recently, some important researches found that one of the most significant reasons for the low conductivity of HEMs is the lack of microphase separation structure, which promotes continuous ionic aggregation and ionic nanochannels formation to provide pathways for ion conduction, since the membranes were cast in their nonionic form [8,9]. Yan and Hickner have recently reported the relationship between the conductivity and the amination types of the HEMs [10]. Their findings suggest that ionic interactions during the casting process can promote ionic aggregation. The membranes prepared by casting the polymer previously converted to the ionic form, homogeneous amination, had higher conductivity than those cast in nonionic form and subsequently converted to ionic form, heterogeneous amination, indicating the importance of building an efficient microphase separation structure to improve the membrane performance. This requirement is supported by Coates and co-workers who prepared HEMs by introducing tetraalkylammonium groups to the monomer prior to the polymerization and film-casting processes [6,11,12], and Zhuang's groups who prepare HEMs by converting the polymer solution to quaternary-ammonium-ionic form and then casting films [13,14]. However, due to the restriction of the traditional film-casting method, it is difficult to synthesize HEMs as thin as 10 μm without any loss of mechanical integrity. Considering the mobility of hydroxide ion is inherently slower than that of proton in dilute solution, thinner HEMs are promising due to their decreased ionic resistance, and as a result, increased fuel cell performance [8,12]. Plasma polymerization method was used to synthesize membrane for fuel cells [15–17]. More recently,

* Corresponding author. Tel.: +86 551 5591378; fax: +86 551 5591310.
E-mail address: hujue@ipp.ac.cn (J. Hu).

0378-7753/$ – see front matter © 2011 Elsevier B.V. All rights reserved.
doi:10.1016/j.jpowsour.2011.09.089

we have prepared HEMs by the plasma polymerization approach [18–22]. Although the plasma polymerized HEMs possess ultra-thin and mechanical integrity structure, the synthesis of HEM with efficient microphase separated structure is restricted due to the heterogeneous amination and the catalyst poisoning problem still exists in the post-quaternization process [21]. Herein, plasma copolymerization was adopted to synthesize HEMs.

In the plasma copolymerization process, exciting species such as electrons, ions and neutral particles within plasma bombard with the monomers and create active sites for quaternization and polymerization, and then the plasma polymers with quaternary ammonium groups deposit onto the substrate forming solid-state membrane. By employing the plasma copolymerization approach from the monomers with benzyl chloride and tertiary amine moiety, HEM synthesis can be greatly simplified and the problem of catalyst poisoning is expected to be resolved since the post-quaternization is unnecessary [21]. This approach enabled a homogeneous amination and led to a good microphase separation structure in the anion exchange membrane. In addition, the membrane can be directly deposited onto the catalyst layer leading to maximization of the catalyst/electrolyte interface, and as a result, an efficient three-phase boundary and low interfacial resistance between membrane and electrodes [21]. Furthermore, the highly cross-linked structure can improve the chemical and mechanical properties of membrane [20,23]. There has hitherto been no report of HEMs comprehensively possessing the excellent microphase separation and ultra-thin structure with mechanical integrity, as well as the ability of building an efficient three-phase-boundary without the need of solubilizing the polymer in low boiling point water-soluble solvents.

2. Experimental

2.1. Materials

4-Vinylbenzyl chloride (VBC, 95 wt%) and 4-vinyl pyridine (VP, 95 wt%) were purchased from Alfa Aesar®, and used without further purification. Potassium hydroxide (KOH, AR grade), sodium hydroxide (NaOH, AR grade), hydrochloric acid (HCl, 37 wt%) were obtained from Shanghai Chemical Reagent Store (China). AHA membrane (Cl^- form) received from NEOSEPTA was treated with 2 M KOH solution to convert the Cl^- form into OH^- form, and then stored in deionized water. Deionized water was used in all experiments.

2.2. Synthesis of plasma-copolymerized hydroxide exchange membrane

In the present study, 4-vinyl pyridine (VP) and 4-vinylbenzyl chloride (VBC) were used as monomers to synthesize plasma-copolymerized HEMs with quaternary ammonium chloride groups (PCPNCl), followed by hydroxide exchange to preparation HEMs with quaternary ammonium hydroxide groups (PCPNOH), as shown in Scheme 1. The reactor was in a after-glow discharge configuration, meaning that the glow discharge was produced in the upper part of the reactor (in a Pyrex glass tube) and the plasma polymerization was performed in the lower part of it (stainless steel chamber). The plasma discharge was sustained by a pulsed mode RF power supply between two external electrodes (5 cm gap) in the Pyrex glass tube using argon (supplied by Air liquid) as working gas. 4-Vinylbenzyl chloride (VBC) and 4-vinyl pyridine (VP) monomers carried by H_2 (supplied by Air liquid), were introduced into the polymerization region through air distribution rings. The flow rates of VBC, VP, H_2 and Ar were controlled by gas mass flow controllers. The partial pressure ratio between vinyl pyridine and vinylbenzyl chloride was kept constant at 1:1. The constant parameters in this experiment were 20 W for the discharge power, 60 Pa for the reactor total pressure (10 Pa for partial pressure of argon) and −10 V for the bias voltage to the substrate. There are different substrates used to support plasma-polymerized membrane: silicon wafers [P-doped Si(1 0 0)] for SEM observations, stainless steel plates for chemical structural characterizations and polytetrafluoroethylene (PTFE) porous substrates for thermal stability and ionic conductivity measurements.

The plasma-polymerized membranes (PCPNCl) were immersed in 2 mol L^{-1} potassium hydroxide aqueous solution at room temperature for 48 h to convert the Cl^- form into OH^- form. Then, the alkalized membranes (PCPNOH) were washed by deionized water to remove any trapped potassium hydroxide and finally immersed in deionized water >48 h with frequent water changes.

2.3. Characterization of membranes

The morphology and microstructure of the plasma polymerized membrane were studied by scanning electron microscope (SEM) and transmission electron microscope (TEM). Before SEM (Sirion 200, FEI, at operation voltage of 5.0 kV) observation, the PCPNOH membrane with silicon substrate was frozen in liquid nitrogen and broken to expose the cross-section. For TEM analysis, a piece of PCPNCl membrane sample (Cl^- form) was embedded in epoxy resin at 60 °C for 8 h. The sample was then ultramicrotomed on a using a microtome (Leica Ultracut) to a thickness of ~90 nm and placed on a 200 mesh copper grid. Images were taken on JEM-2100 (Japan) at 200 kV.

The XPS analysis was carried out using a Thermo ESCALAB 250 spectroscopy (Thermo Electron Corporation) at a power of 150 W with a monochromatic Al Kα radiation at 1486.6 eV. XPS of PCPNCl and PCPNOH membranes were recorded at pass energies of 70 eV for survey spectra and 20 eV for core level spectra. The spectrometer energy scale calibration was checked by setting Ag $3d_{5/2}$ = 368.26 eV and the spectra were calibrated with respect to the C 1s peak at 284.6 eV.

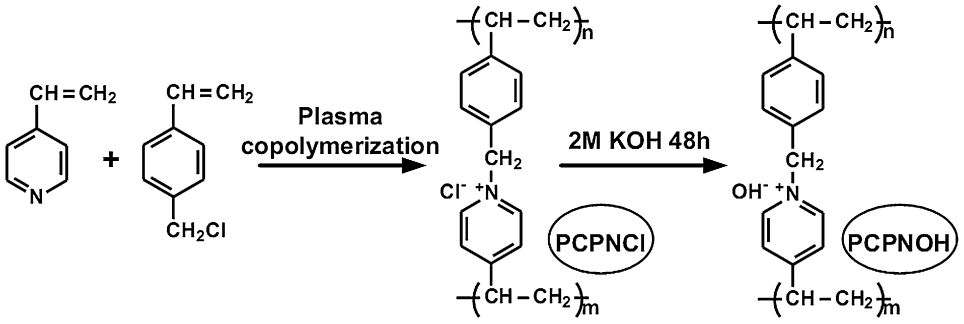

Scheme 1. Synthesis of plasma copolymerized hydroxide exchange membranes containing quaternary ammonium groups (PCPNOH).

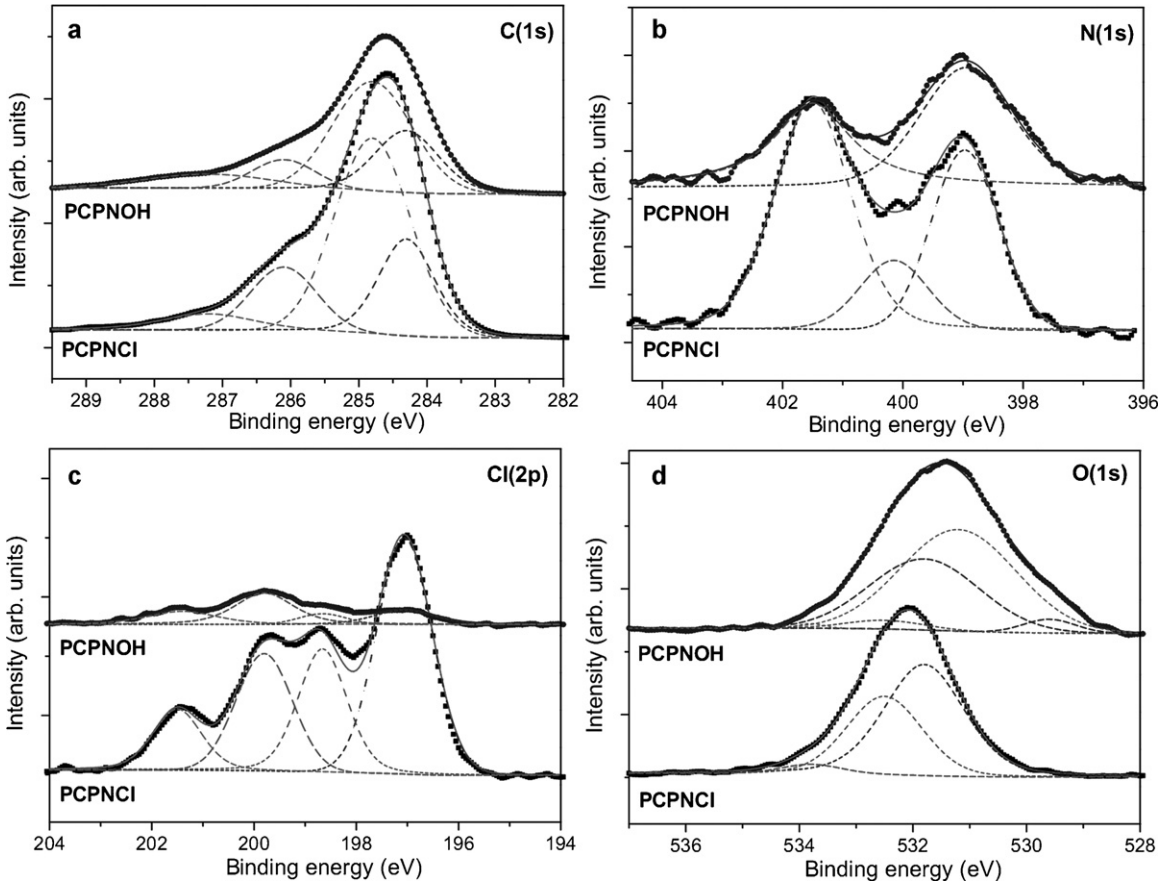

Fig. 1. X-ray photoelectron spectroscopy (XPS) [C 1s (a), N 1s (b), Cl 2p (c) and O 1s (d)] spectra of PCPNCl and PCPNOH.

Thermal degradation and stability of the membranes were investigated using differential scanning calorimetry (DSC) (Q2000, TA, USA). ~2 mg dried membrane sample with PTFE substrate, placed in a Pt crucible, was heated from ambient temperature to 350 °C under flowing nitrogen at the scanning rate of 5 °C min^{-1}.

2.4. Ion-exchange capacity and ionic conductivity measurements

The ion-exchange capacities (IECs) of PCPNCl and PCPNOH membranes were measured by classical back titration method. The hydroxide conductivity of the obtained membrane was measured by three-electrode AC impedance spectroscopy. The measurement details have been reported in our previous work [19,20], shown in the supplementary information.

3. Results and discussion

The generation of the quaternary ammonium moiety in plasma copolymerized membrane (PCPNCl) can be indicated by the absorption at ~1488 cm^{-1} assigned to C–H bending of quaternary ammonium, ~1648 cm^{-1} attributed to amide band of ATR-FTIR spectra, shown in Fig. S1 [24–27]. The chemical structure of the PCPNCl and PCPNOH membranes were further analyzed by X-ray photoelectron spectroscopy (XPS), shown in Fig. 1. As regards the C 1s spectra, there are four peaks in plasma-copolymerized anion exchange membranes, which appear at 284.3 eV for C=C, 284.8 eV for C–C, C–H, 286.1 eV for C–Cl, C=N, C–O, and 287.1 eV for C–N, C=O [28–30]. The existence of quaternary ammonium groups in PCPNCl membrane can be demonstrated by the decomposition of N 1s spectrum (pyridinic N at 398.9 eV, pyrrolic N at 400.1 eV and quaternary N at 401.5 eV), shown in Fig. 1b, indicating successful conversion of ionic form during the plasma copolymerization process [30]. Quantitatively analysis of the N 1s spectra, shown in Table 1, reveals that the percentage of quaternary nitrogen is 2.41 at.% and 1.27 at.% for PCPNCl and PCPNOH membranes, respectively, which are higher than that of sulphur in sulfonic acid groups for Nafion 117 membrane (shown as 1.23 at.% in Ref. [25]), indicating a high hydroxide ion conductivity in the plasma-copolymerized HEMs. Table 1 also shows the atomic percentage of carbon, nitrogen, chlorine and oxygen in PCPNCl and PCPNOH membranes. The atomic percentage of chlorine decreases after the alkalization process, while the percentage of oxygen increase, suggesting the conversion of quaternary ammonium chloride groups into quaternary ammonium hydroxide groups. This can be further demonstrated by the core level XPS spectra of Cl 2p and O 1s, as shown in Fig. 1c and d, where the intensity peaks characteristic of Cl^- (at 197.0 eV) decreased, but those characteristics of OH^- (at 531.2 eV) increased [31,32].

The hydroxide conductivity of the PCPNOH membrane is plotted as a function of temperature over the range of 20–60 °C at 100% relative humidity (RH) (Fig. 2). For comparison, the hydroxide conductivity of the commercial AHA–OH membrane (NEOSEPTA® AHA membrane OH^- form) was also measured under the same conditions. The PCPNOH membrane (1.29 mmol g^{-1}) exhibits excellent hydroxide conductivity of 13.7 mS cm^{-1} at 20 °C (see Fig. S2 of Nyquist plot), which is 3.9 times that of the AHA–OH membrane

Table 1
XPS elemental analysis of plasma-copolymerized PCPNCl and PCPNOH membranes.

Membrane	C (at.%)	O (at.%)	Cl (at.%)	N (at.%)	N^+ (at.%)
PCPNCl	85.38	11.28	2.71	4.54	2.41
PCPNOH	79.40	19.58	0.86	2.85	1.27

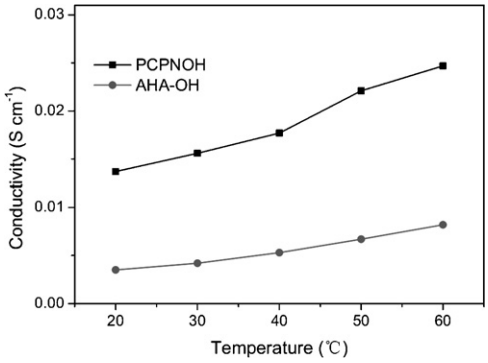

Fig. 2. Temperature dependence of the hydroxide ion conductivity of PCPNOH and AHA membranes.

(3.5 mS cm^{-1}). The ionic conductivity of PCPNOH membrane is on the order of 10 mS cm^{-1} at room temperature indicating the satisfactory for application of the membrane in fuel cells [33]. At the same time, the ionic conductivity increased with increasing temperature, and increased to 24.7 mS cm^{-1} at 60 °C, which is high compared with that of many other types of HEMs such as quaternized poly(ether-imide) (3.3 mS cm^{-1} at 60 °C) [34], quaternized cardo polyetherketone (5.1 mS cm^{-1} at 60 °C) [35], and tetraalkylammonium-functionalized poly(arylene ether sulfone) (18 mS cm^{-1} at 60 °C) [36]. The good conductivity, we surmise, is because of the aggregation of ionic groups and well-connected ion transport pathways in the plasma-copolymerized membranes. In order to investigate hydrophilic/hydrophobic microphase separation and the ion transport channel on the membrane, transmission electron micrograph (TEM) observations were carried out (Fig. 3).

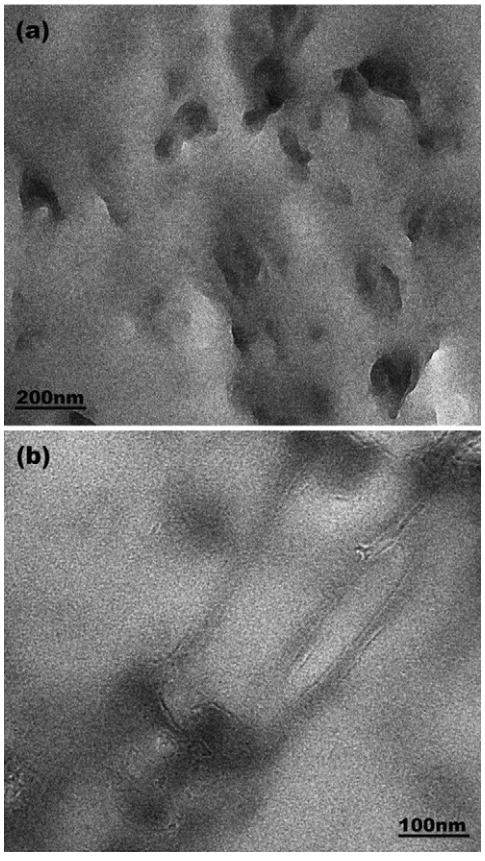

Fig. 3. (a) TEM image of the PCPNCl membrane and (b) TEM image of the cross-section of PCPNCl membrane.

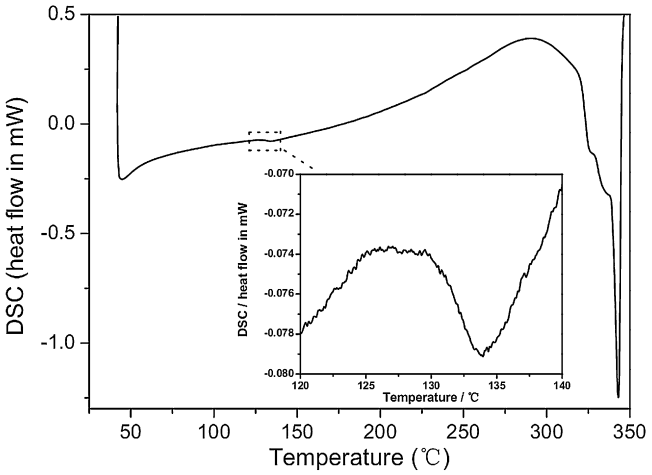

Fig. 4. DSC analysis of the PCPNOH membrane with the PTFE substrate.

TEM micrographs reveal the presence of ionic domains and ionic channels in the plasma-copolymerized PCPNCl membrane matrix due to the difference of electronic density between hydrophobic backbone and ionic domain [11,37]. As can be seen in Fig. 3a, the ionic clusters (the dark areas) are well distributed in the hydrophobic backbones (the bright areas). These ionic clusters can be connected to form ion transport channels. From the cross-sectional view of PCPNCl membrane, as shown in Fig. 3b, the ionic channels can be clearly observed. The excellent phase-separated morphology of the PCPNCl membrane indicates that the plasma copolymerization allowed the generation and aggregation of ionic groups and the formation of ionic transport channels in the solid-state membrane, which is thought to be essential for high ionic conductance.

Polymers which full contact with the catalyst layer hold great promise as HEMs because the maximization of catalyst/electrolyte interface can conduce to forming an efficient three-phase-boundary (TPB) structure. Fig. S3 shows the SEM images of the PCPNOH membrane deposited on silicon wafer, where a flat, dense, uniform and undamaged structure with a thickness of 3.4 μm can be seen. The plasma-copolymerized HEMs could completely cover the substrate and did not peel off from it after immersion in 2 M KOH solution and deionized water for several days, indicating a strong adhesion between the membrane and substrate. These results are crucial for preparing fuel cells with efficient TPB and low interfacial resistance between membrane and electrodes. It is unfeasible for other HEMs synthesis methods to build efficient TPB in the absence of quaternary-amine-functionalized polymer solution. The SEM image displays the undamaged membrane structure in 2 M KOH solution for 2 days, indicating the high chemical stability of the obtained membrane [14]. The thermal stability of PCPNOH membrane deposited on PTFE substrate was investigated by differential scanning calorimetry (DSC) in flowing nitrogen. The decomposition temperature of quaternary ammonium observed from Fig. 4 is 130 °C, indicating the steady operation of PCPNOH membrane below 100 °C, which is higher than the typical HEMFC working temperature, *i.e.* 60–70 °C. The thermal stability of the plasma copolymerized HEM was acceptable [14].

4. Conclusion

We have successfully developed a new approach for HEMs synthesis. The plasma copolymerization allowed the generation and aggregation of ionic groups and the formation of ionic transport channels, leading to an excellent phase-separated morphology of the PCPNCl membrane. The plasma copolymerized HEMs

displayed excellent hydroxide ion conductivity (13.7 mS cm^{-1} at 20 °C), chemical and thermal stability, as well as the ability of building an efficient three-phase-boundary, making them very exiting candidates for fuel cell applications. The novel plasma copolymerization approach casts a new light on the conceptual and methodological improvement in designing fuel cells.

Acknowledgements

This research is financially supported by the Institute of Plasma Physics, Chinese Academy of Sciences (No. Y05FCQ1128; No. 095GZ1156Y), the National Nature Science Foundation of China (No. 11175214; No. 10975162) and the Core-University program of Japan–China.

Appendix A. Supplementary data

Supplementary data associated with this article can be found, in the online version, at doi:10.1016/j.jpowsour.2011.09.089.

References

[1] R. Borup, J. Meyers, B. Pivovar, Y.S. Kim, R. Mukundan, N. Garland, D. Myers, M. Wilson, F. Garzon, D. Wood, P. Zelenay, K. More, K. Stroh, T. Zawodzinski, J. Boncella, J.E. McGrath, M. Inaba, K. Miyatake, M. Hori, K. Ota, Z. Ogumi, S. Miyata, A. Nishikata, Z. Siroma, Y. Uchimoto, K. Yasuda, K.C. Kimjima, N. Iwashita, Chem. Rev. 107 (2007) 3904–3951.
[2] J.R. Varcoe, R.C.T. Slade, Fuel Cells 5 (2005) 187–200.
[3] M. Ünlü, J. Zhou, P.A. Kohl, Angew. Chem. Int. Ed. 49 (2010) 1299–1301.
[4] B. Lin, L. Qiu, J. Lu, F. Yan, Chem. Mater. 22 (2010) 6718–6725.
[5] J.R. Varcoe, R.T.C. Slade, E.L.H. Yee, Chem. Commun. 42 (2006) 1428.
[6] T.J. Clark, N.J. Robertson, H.A. Kostalik Iv, E.B. Lobkovsky, P.F. Mutolo, H.D. Abruña, G.W. Coates, J. Am. Chem. Soc. 131 (2009) 12888–12889.
[7] O. Diat, G. Gebel, Nat. Mater. 7 (2008) 13–14.
[8] M.R. Hibbs, M.A. Hickner, T.M. Alam, S.K. McIntyre, C.H. Fujimoto, C.J. Cornelius, Chem. Mater. 20 (2008) 2566–2573.
[9] K. Schmidt-Rohr, Q. Chen, Nat. Mater. 7 (2008) 75–83.
[10] J. Yan, M.A. Hickner, Macromolecules 43 (2010) 2349–2356.
[11] N.J. Robertson, H.A. Kostalik, T.J. Clark, P.F. Mutolo, H.D. Abruna, G.W. Coates, J. Am. Chem. Soc. 132 (2010) 3400–3404.
[12] H.A. Kostalik, T.J. Clark, N.J. Robertson, P.F. Mutolo, J.M. Longo, H.c.D. Abruña, G.W. Coates, Macromolecules 43 (2010) 7147–7150.
[13] J. Pan, Y. Li, L. Zhuang, J. Lu, Chem. Commun. 46 (2010) 8597–8599.
[14] J. Pan, S. Lu, Y. Li, A. Huang, L. Zhuang, J. Lu, Adv. Funct. Mater. 20 (2010) 312–319.
[15] A. Ennajdaoui, S. Roualdes, P. Brault, J. Durand, J. Power Sources 195 (2010) 232–238.
[16] M. Schieda, S. Roualdès, J. Durand, A. Martinent, D. Marsacq, Desalination 199 (2006) 286–288.
[17] K. Matsuoka, S. Chiba, Y. Iriyama, T. Abe, M. Matsuoka, K. Kikuchi, Z. Ogumi, Thin Solid Films 516 (2008) 3309–3313.
[18] J. Hu, Y. Meng, C. Zhang, S. Fang, Thin Solid Films 519 (2011) 2155–2162.
[19] J. Hu, C. Zhang, J. Cong, H. Toyoda, M. Nagatsu, Y. Meng, J. Power Sources 196 (2011) 4483–4490.
[20] C. Zhang, J. Hu, J. Cong, Y. Zhao, W. Shen, H. Toyoda, M. Nagatsu, Y. Meng, J. Power Sources 196 (2011) 5386–5393.
[21] C. Zhang, J. Hu, Y. Meng, M. Nagatsu, H. Toyoda, Chem. Commun. (2011), doi:10.1039/c1cc11888a.
[22] C. Zhang, J. Hu, M. Nagatsu, Y. Meng, W. Shen, H. Toyoda, X. Shu, Plasma Process. Polym. (2011), doi:10.1002/ppap.201000197.
[23] H. Yasuda, Plasma Polymerization, 1st ed., Acadamic Press, Inc., Orlando, FL, 1985.
[24] N. Sundaraganesan, H. Saleem, S. Mohan, M. Ramalingam, V. Sethuraman, Spectrochim. Acta A 62 (2005) 740–751.
[25] Z. Jiang, Z. Jiang, X. Yu, Y. Meng, Plasma Process. Polym. 7 (2010) 382–389.
[26] E. Loubaki, M. Ourevitch, S. Sicsic, Eur. Polym. J. 27 (1991) 311–317.
[27] Y. Yamaguchi, T.T. Nge, A. Takemura, N. Hori, H. Ono, Biomacromolecules 6 (2005) 1941–1947.
[28] D. Briggs, G. Beamson, Anal. Chem. 64 (1992) 1729–1736.
[29] T.I.T. Okpalugo, P. Papakonstantinou, H. Murphy, J. McLaughlin, N.M.D. Brown, Carbon 43 (2005) 153–161.
[30] Y. Wang, Y. Shao, D.W. Matson, J. Li, Y. Lin, ACS Nano 4 (2010) 1790–1798.
[31] S.B. Roscoe, S. Yitzchaik, A.K. Kakkar, T.J. Marks, Z.Y. Xu, T.G. Zhang, W.P. Lin, G.K. Wong, Langmuir 12 (1996) 5338–5349.
[32] U. Sulaeman, S. Yin, T. Sato, Appl. Phys. Lett. 97 (2010) 103102–103103.
[33] T.N. Danks, R.C.T. Slade, J.R. Varcoe, J. Mater. Chem. 13 (2003) 712–721.
[34] G. Wang, Y. Weng, D. Chu, D. Xie, R. Chen, J. Membr. Sci. 326 (2009) 4–8.
[35] Y. Xiong, Q.L. Liu, Q.H. Zeng, J. Power Sources 193 (2009) 541–546.
[36] J. Wang, Z. Zhao, F. Gong, S. Li, S. Zhang, Macromolecules 42 (2009) 8711–8717.
[37] S. Livi, J.F. Gerard, J. Duchet-Rumeau, Chem. Commun. 47 (2011) 3589–3591.